JBC RESEARCH ARTICLE

Strength of Cu-efflux response in *Escherichia coli* coordinates metal resistance in *Caenorhabditis elegans* and contributes to the severity of environmental toxicity

Received for publication, February 10, 2021, and in revised form, July 29, 2021 Published, Papers in Press, August 8, 2021,
https://doi.org/10.1016/j.jbc.2021.101060

Catherine M. Shafer[1], **Ashley Tseng**[2], **Patrick Allard**[1,2,3,*], **and Megan M. McEvoy**[1,2,3,4,*]

From the [1]*Molecular Toxicology Interdepartmental Program,* [2]*Molecular Biology Institute,* [3]*Institute for Society and Genetics,* [4]*Department of Microbiology, Immunology and Molecular Genetics, University of California, Los Angeles, Los Angeles, California, USA*

Edited by Ursula Jakob

Without effective homeostatic systems in place, excess copper (Cu) is universally toxic to organisms. While increased utilization of anthropogenic Cu in the environment has driven the diversification of Cu-resistance systems within enterobacteria, little research has focused on how this change in bacterial architecture impacts host organisms that need to maintain their own Cu homeostasis. Therefore, we utilized a simplified host–microbe system to determine whether the efficiency of one bacterial Cu-resistance system, increasing Cu-efflux capacity *via* the ubiquitous CusRS two-component system, contributes to the availability and subsequent toxicity of Cu in host *Caenorhabditis elegans* nematode. We found that a fully functional Cu-efflux system in bacteria increased the severity of Cu toxicity in host nematodes without increasing the *C. elegans* Cu-body burden. Instead, increased Cu toxicity in the host was associated with reduced expression of a protective metal stress-response gene, *numr-1*, in the posterior pharynx of nematodes where pharyngeal grinding breaks apart ingested bacteria before passing into the digestive tract. The spatial localization of *numr-1* transgene activation and loss of bacterially dependent Cu-resistance in nematodes without an effective *numr-1* response support the hypothesis that *numr-1* is responsive to the bacterial Cu-efflux capacity. We propose that the bacterial Cu-efflux capacity acts as a robust spatial determinant for a host's response to chronic Cu stress.

Bacteria define an organism's relationship with the environment. Their presence in a host at all three major routes of environmental exposure (dermal, respiratory, digestive) broadly impacts drug metabolism and efficacy (1–3), pathogenicity (4), nutrient biosynthesis (5), and disease progression (6–9). However, the effects of bacterial activity on a host's response to toxicant exposure are only beginning to be examined (10). One such toxicant the environmental excess of which elicits conserved homeostatic responses in prokaryotes (11–13) and eukaryotes (14) alike is copper (Cu), an essential transition metal recognized by the Agency of Toxic Substances and Disease Registry (ATSDR) for its ability to catalyze Fenton-like reactions, displace metal cofactors lower on the Irving-Williams series, and oxidize lipids when too much is present in the environment (15–17). In conditions of excess Cu, toxicity can develop rapidly and coincide with the development of disease pathology if an organism's homeostatic responses fail to correct the situation (18, 19).

However, little is known about how challenged prokaryotic and eukaryotic systems interact. Outside generalized treatments that limit overall bacterial density (20), how specific bacterial activity contributes to homeostatic responses in the host has yet to be examined. Diversification rates in enterobacteria suggest that Cu-efflux systems are under considerable selective pressure from increasing anthropogenic Cu deposition in the environment (21, 22). Furthermore, research from the human microbiome project has found that bacterial activity involved in metal detoxification, such as increasing Cu-efflux capacity, is indeed a ubiquitous component of the digestive microbiome today (23). The pervasiveness and necessity of bacterial Cu-efflux systems at major sites of eukaryotic Cu-uptake, like the digestive tract, compel a more thorough investigation into how specific bacterial responses contribute to the development of Cu toxicity in host organisms.

Previous work in our lab (24–26) developed strains of *Escherichia coli* with variable Cu-efflux capacities as measured by quantifying their Cu accumulation. Targeted deletions in genes for a Cu-handling system, CusRS, within a Cu oxidase (*cueO*) deletion background maximized the Cu(I) interaction with Cu(I)-specific CusRS and produced mutants with approximately 50 and 25% Cu-efflux capacity compared with *E. coli* with *ΔcueO* alone (100%*WT*) (26). CusRS is a conserved two-component system (TCS) composed of a Cu(I) histidine kinase sensor (CusS) and response regulator (CusR) (24). The combined action of this sensor and response regulator drives the expression of a Cu-efflux pump, CusCFBA, with a narrow substrate range that selectively removes excess periplasmic Cu(I) (27) (Fig. 1). We hypothesized that alterations in bacterial Cu removal would modify the availability and subsequent toxicity of Cu in a simplified host–microbe system.

* For correspondence: Megan M. McEvoy, mcevoymm@ucla.edu; Patrick Allard, pallard@ucla.edu.

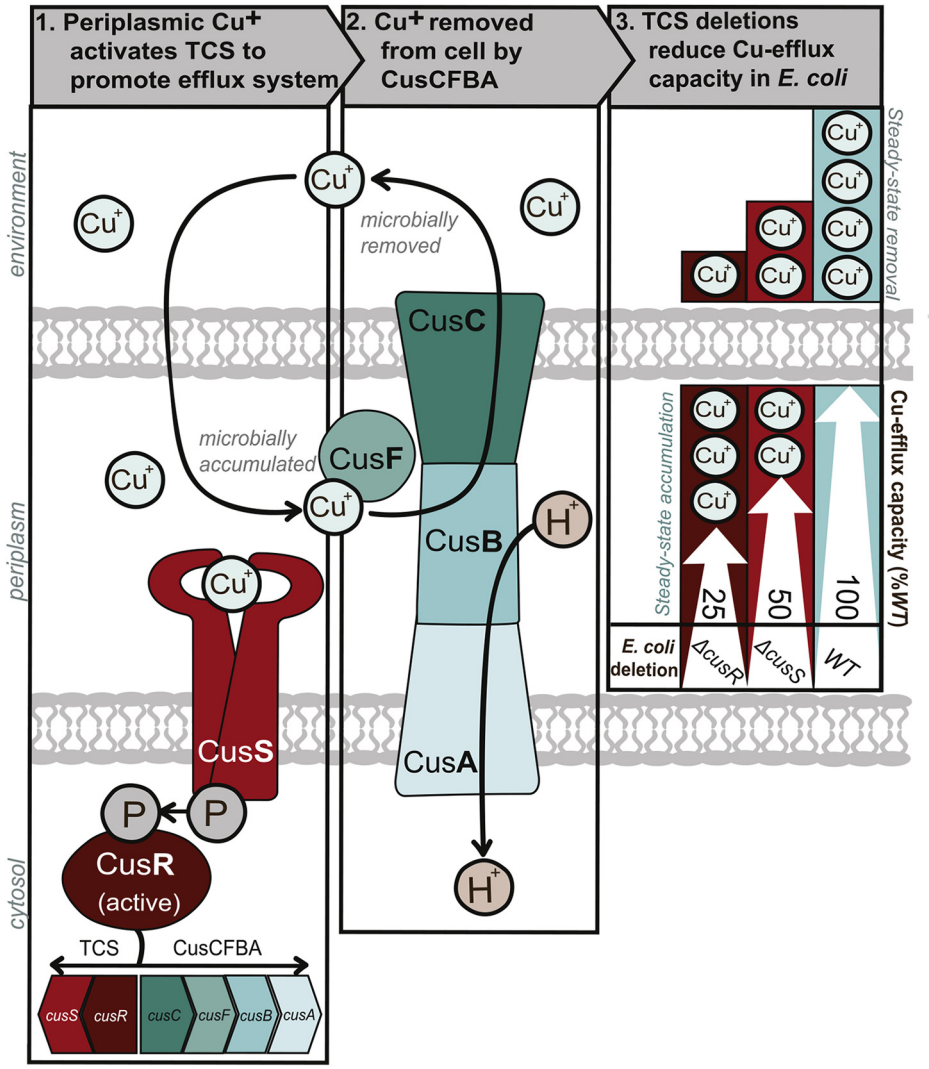

Figure 1. CusRS regulates Cu-efflux capacity in an *E. coli* model system. Cross section of *E. coli* showing a response system that deals with Cu^+ excess in the environment. Removal of excess Cu^+ by bacteria is dependent upon (1) activation of a TCS that responds to Cu^+ in the periplasm. Signal transduction from the periplasmic domain of CusS, a histidine kinase, to the cytosol leads to temporary phosphorylation and activation of CusR, which promotes expression of the *cus* operon. 2, expression of the *cus* operon drives increased efficiency in the removal of periplasmic Cu^+ *via* the CusCFBA antiporter. 3, targeted deletions of the genes for the CusS-CusR TCS within a periplasmic copper oxidase (*ΔcueO*) background increase the ratio of accumulated Cu^+ to removed Cu^+ by varying degrees.

Caenorhabditis elegans (*C. elegans*), a soil-dwelling nematode that thrives on single-culture *E. coli* lawns in laboratory conditions, is a well-established model for studying conserved host–microbe interactions involved in Cu homeostasis and detoxification (4, 28–30). Evidence for conserved Cu-homeostatic elements is found in orthologs for a passive Cu-uptake transporter (31) and the active Cu exporter ATP7A/B (32), which are both expressed along the nematode's digestive tract, mirroring the expression patterns and physiology of higher organisms (14, 20). Under Cu stress, nematodes also present dose-dependent Cu-toxicity responses that encompass developmental, behavioral, reproductive, and aging trajectories, which may be influenced by bacterial activity (33–40). Furthermore, these responses to metal stress are often consistent and conserved across species, allowing for a detailed investigation of host stress responses mediated by bacterial activity. For instance, activation of heat-shock factor 1 following metal toxicity is observed in both humans and nematodes (41, 42), which is signaled in *C. elegans* by the activation of a nuclear-localized metal-responsive gene (*numr-1*) and is proposed to influence RNA splicing in response to impaired RNA-processing machinery during metal stress (42).

Using this *C. elegans*/*E. coli* host–microbe system, we show that an increase in bacterial Cu-efflux, through the activity of CusRS, alters the magnitude and spatial distribution of *numr-1* activation and sensitizes the host to environmental Cu over time. Despite increasing sensitivity to equimolar Cu exposures, the overall host Cu-body burden did not account for the increasing toxicity in the host. Taken together, these findings reveal how a ubiquitous bacterial response, selected for through persistent anthropogenic Cu release over generations, establishes the spatial distribution and efficiency of Cu detoxification in a host model.

Results

A simplified exposure paradigm to test the impact of bacterial Cu-efflux capacity on host Cu sensitivity

We first assessed common Cu-toxicity endpoints observed in *C. elegans* as hallmarks of Cu stress coping mechanisms to determine whether they could be influenced by the bacterial Cu-efflux capacity in the environment. To this aim, we used a simplified exposure paradigm for the *C. elegans*/*E. coli* host–microbe system that, first, used no (0 μM) or excess (100 μM) exogenous Cu concentrations that did not strongly impair bacterial growth rate (Fig. S1*A*) or plate density (Fig. S1*B*) to ensure that the CusRS response could be active at the same molarity at which *C. elegans* Cu toxicity is observed (32). Second, Cu exposure to *C. elegans* was limited to developmentally synchronous populations that excluded early developmental stress responses that can confound the severity of toxicity endpoints (32, 39). As described below, this experimental exposure paradigm allowed us to clearly distinguish the impact of varying bacterial Cu-efflux capacity on the *C. elegans* host sensitivity to Cu stress.

The physiological response to environmental challenges can vary greatly across *C. elegans* developmental stages (39). Therefore, multiple, specific dose-dependent chronic Cu-toxicity endpoints were originally selected to capture adverse outcomes on two central biological processes: aging and reproduction (Fig. 2*A*). Initially, all endpoints were assessed for their sensitivity to 100 μM Cu in the presence of bacteria with 100%*WT* Cu-efflux capacity (control). Across their life span, nematode populations exposed to 100 μM Cu on 100%*WT* control bacteria experienced a 41% reduction in median life span (Fig. 2*B*, thick blues lines, $p < 0.0001$, log-rank Mantel–Cox test), from 14.5 days to 8.5 days, when compared with those exposed to 0 μM Cu in the media. The decreased

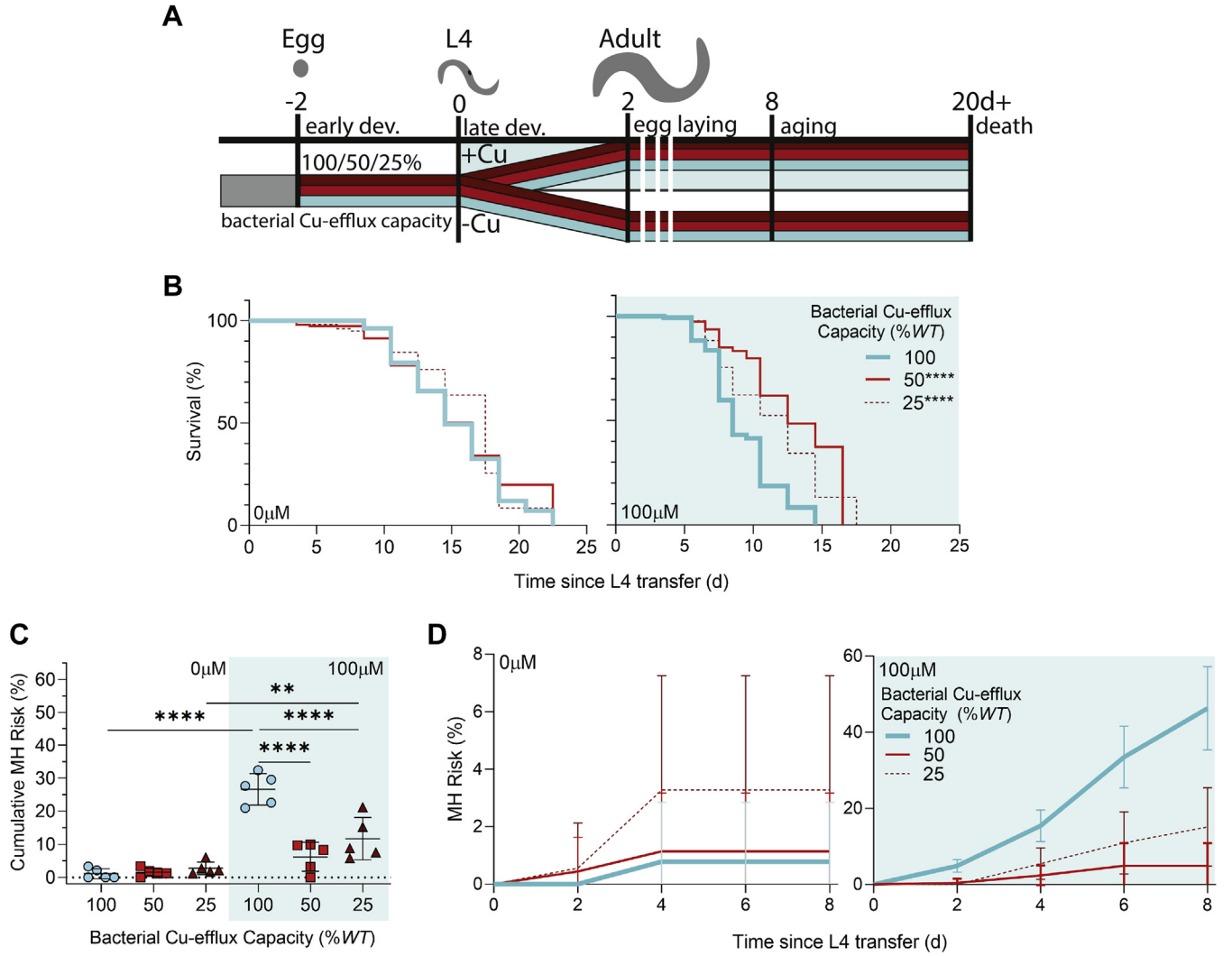

Figure 2. Host sensitivity to chronic Cu excess is dependent on bacterial Cu-efflux capacity. *A*, experimental design. For chronic exposures, adults were transferred to new plates at least every 48 h after initial L4 transfer. *B*, Kaplan–Meier lifespan analysis with 0 μM or 100 μM Cu. Significance between life span data was calculated using a Mantel–Cox log-rank test (N = 3–4, n > 50) where ****$p < 0.0001$. *C*, cumulative incidence MH risk through reproductive life span in *N2* nematodes (N = 5, n = 62–121). Each symbol on a graph denotes the average of one experimental replicate composed of at least 60 nematodes. *D*, MH incidence risk analysis was performed on nematodes exposed to 0 μM or 100 μM Cu over time. *Shaded regions* on graphs highlight conditions of excess Cu. Significance was determined using a two-way ANOVA with Tukey's multiple comparison's test where **$p \leq 0.01$, ****$p < 0.0001$, and error bars mark the upper and lower SD from calculated mean.

survival of *C. elegans* exposed to 100 μM Cu confirms the sensitivity of median life span analysis to Cu.

To test whether nematode Cu toxicity also impacted earlier life events in our simplified exposure paradigm, we monitored the reproductive period—where active egg laying takes place (Fig. 2*A*)—by assessing *C. elegans* neuromuscular inability to lay eggs over time, resulting in Matricidal Hatching (MH), and the total number of viable eggs laid (average viable brood size) over the same period. MH, when the offspring of hermaphroditic nematodes hatch inside the parent without being expelled from the vulva, is a response to environmental stress that increased by 25.4% (Fig. 2*C*, blue circles, $p > 0.0001$, two-way ANOVA with Tukey's multiple comparisons) on 100%*WT* control bacteria when 100 μM Cu exposures are compared with 0 μM Cu exposures. Furthermore, this trend became more pronounced in the later reproductive period (Fig. 2*D*, thick blue lines). In contrast, over the same reproductive period (Fig. S2*A*), cumulative brood size was unaffected by the presence of 100 μM Cu. Further analysis found that brood size was not significantly reduced by the addition of Cu in any bacterial condition tested (Fig. S2*B*), indicating that any bacterially dependent variation in brood size appears independent of Cu stress in our simplified exposure paradigm. Taken together, these results identify MH, but not brood size, as a responsive and sensitive endpoint reflective of Cu stress.

To better understand the discrepancy between MH and brood size in response to Cu stress, we also investigated the impact of Cu exposure on the nematode germline. While DAPI-stained germlines early in the reproductive period showed some reduced proliferation of germline nuclei indicative of developmental delay (43) (average number of nuclei across in 0 μM Cu is 10, but only 8 in 100 μM Cu) (Fig. S2, *C* and *D*), there were no strong indicators of acute germline toxicity such as nuclear gaps or DNA aggregates, which correlate with embryonic lethality and precede reductions in the viable brood size (44) independent of MH. These results suggest that germline toxicity does not contribute to the Cu toxicity observed in *C. elegans* either because this endpoint is less sensitive to Cu stress, as has previously been observed (38), or is more dependent on early developmental exposures.

Role for bacterial Cu-efflux capacity in host toxicity endpoints

Next, we used the two Cu-sensitive endpoints, life span and MH, to test whether an impaired bacterial Cu-efflux capacity modifies the *C. elegans* host response to the addition of 100 μM Cu in the media. Lifespan assays revealed that nematode populations on bacterial lawns with reduced Cu-efflux capacity (25% or 50% of normal Cu-efflux) exhibited increased median survival compared with those grown with 100%*WT* control bacteria, increasing 47% from 8.5 days to 12.5 days ($p < 0.0001$, log-rank Mantel–Cox test) (Fig. 2*B*). MH is similarly improved by reduced bacterial Cu-efflux; 50%*WT* Cu-efflux capacity during Cu stress resulted in a reduced cumulative population risk of just 6.2 ± 4.4% compared with 27 ± 4.8% on 100%*WT* control bacteria ($p < 0.0001$, two-way ANOVA with Tukey's multiple comparisons) while 25%*WT* Cu-efflux capacity reduced cumulative risk of MH by over half of the risk compared with control bacterial lawns (11.7 ± 6.4 *versus* 27 ± 4.8, respectively $p = 0.0025$, two-way ANOVA with Tukey's multiple comparisons) during exposure to 100 μM Cu (Fig. 2*C*).

We further assessed whether *E. coli* with impaired bacterial Cu-efflux capacity could act on *C. elegans* Cu-toxicity endpoints independent of their variable Cu-handling induced by 100 μM Cu, for example, *via* changes to the bacterial nutritional status or pathogenicity (45, 46). In testing the Cu-independent effects of *E. coli* strains with 25% and 50%*WT* Cu-efflux capacity in 0 μM Cu, we found that nematodes raised on bacterial lawns with reduced Cu-efflux capacity did not demonstrate any significant difference from those raised on 100%*WT* control bacteria. Without exogenous Cu, median survival ranged from 14.5 to 17.5 days (Fig. 2*B*, $p = 0.3615$, log-rank Mantel–Cox test) and total cumulative MH ranged from 2.7 ± 1.9 to 1.1 ± 1.5% (Fig. 2*C*, $p = 0.9841$, two-way ANOVA with Tukey's multiple comparisons) with increasing bacterial Cu-efflux capacity. Thus, any variation observed in these Cu-toxicity endpoints during exposures to 100 μM Cu could be directly attributed to the variable bacterial Cu-efflux capacity. Taken together, these experiments indicate that a decrease in bacterial Cu-efflux capacity is correlated with a reduction in two chronic Cu-toxicity endpoints in *C. elegans*.

Temporal dependence of MH on bacterial Cu-efflux capacity

We further examined MH risk and monitored how MH risk changes over time to better distinguish the effects of Cu-dependent and Cu-independent adverse outcomes. In the absence of 100 μM Cu, an early uptick in MH risk is observed in 25%*WT* Cu-efflux capacity; between 48 and 72 h after L4 transfer to the 0 μM exposure condition (Fig. 2*D*). However, this early increase is not observed in the 50 or 100%*WT* Cu-efflux capacity conditions. After 72 h, no further increase in MH risk is observed in any bacterial genetic background without 100 μM Cu in the media (Fig. 2*D*). Part of this Cu-independent discrepancy may lie in the *cusR* deletion unique to 25%*WT* Cu-efflux capacity *E. coli*, which impairs a bacterial H_2O_2 stress response that is activated by CusR independent of Cu stress (45). No such cross talk exists with the *cusS* deletion responsible for the 50%*WT* Cu-efflux capacity *E. coli*. These results suggest that Cu-independent roles in the 25%*WT* Cu-efflux capacity *E. coli* are responsible for an early increase in MH risk.

Conversely, the majority of nematode MH risk associated with bacterial Cu-excess occurs later during the nematode's life span, *i.e.*, at timepoints after 72 h of exposures in 100%*WT* control bacteria (Fig. 2*D*). However, this late MH risk is greatly reduced when the bacterial Cu-efflux capacity is limited to either 50% or 25%*WT*. In fact, no significant variation in MH risk is observed in 50%*WT* Cu-efflux capacity bacterial lawns between 0 μM and 100 μM Cu exposures by the end of the reproductive period (Fig. 2*C*). While starvation or nutrient deprivation can be a contributing factor in the appearance of nematode MH in late development (46), this effect was minimized by 1) transferring nematodes to new bacterial lawns

every 2 days and 2) utilizing Cu concentrations that had no impact on bacterial growth rates or survival (Fig. S1). Therefore, these results suggest that late MH risk is mostly dependent on the bacterial response to Cu stress. The timing of MH risk also suggests that bacterial Cu-efflux capacity acts directly on the neuromuscular function of the vulva where age-related degeneration can result in late MH during periods of Cu excess (46).

Early Cu toxicity does not coincide with Cu-body burden in C. elegans

Earlier developmental exposures to Cu strongly impact the growth of *C. elegans*, manifesting as reduced length and larval arrest at the L3 larval stage (32). The potential for our simplified exposure paradigm to cause growth delays before life span and MH risk becomes significant was suggested by the slight reduction in germline proliferation observed after just 24 h of Cu exposure (Fig. S2, *C* and *D*). Therefore, we assessed whether reduced bacterial Cu-efflux capacity could contribute to the nematode's growth rate during a 48 h exposure to 0 or 100 μM Cu starting at the L4 stage (Fig. 3*A*). While we observed a Cu-dependent decrease in *C. elegans* length on 100%*WT* control bacteria (Fig. 3*B*), the effect on growth was less severe when nematodes were raised on bacterial lawns with 25% or 50%*WT* Cu-efflux capacity: from 890 ± 83 μm on 100%*WT* control to 950 ± 120 ($p = 0.001$, two-way ANOVA with Tukey's multiple comparisons) and 950 ± 97 μm ($p < 0.001$, two-way ANOVA with Tukey's multiple comparisons) respectively. Thus, these results indicate that the impact of Cu on L4 to young adult's growth and the ameliorating effect of reduced bacterial Cu-efflux capacity followed the same trends as later-life endpoints (MH and life span).

Next, we tested whether reduced bacterial Cu-efflux capacity improved the aforementioned *C. elegans* Cu-toxicity endpoints by reducing the overall quantity, or internal dose, of Cu in *C. elegans* following the same 48 h exposure to 100 μM Cu since increases in measured Cu-body burden are consistent indicators of excess metal concentration in the environment and are predictive of dose-dependent toxicity (40). To quantify the *C. elegans* Cu-body burden, nematodes were collected after the limited 48 h exposure (Fig. 3*A*) and washed to ensure that graphite furnace atomic absorption spectroscopy (GFAAS) analysis would capture the nematode Cu-body burden with minimal contamination from bacterially accumulated Cu (Fig. S3). Contrary to expectations, we found there was no significant reduction in Cu-body burden in nematodes exposed to 100 μM Cu when the bacterial Cu-efflux capacity was reduced (Fig. 3*C*). On the contrary, the Cu-body burden showed a null or inverse trend, depending on the extent of bacterial Cu-efflux capacity reduction. During 100 μM Cu exposures, reducing bacterial Cu-efflux capacity to 25%*WT* increased the overall body burden of the metal to 450 pg/nematode from 300 pg/nematode for worms raised on bacterial lawns with 100%*WT* Cu-efflux capacity ($p = 0.0150$, two-way ANOVA with Tukey's multiple comparisons) while raising nematodes on 50%*WT* Cu-efflux capacity bacteria did not significantly increase the Cu-body burden compared with 100%*WT* control bacteria. These results indicate that bacterially dependent improvements in nematode Cu-toxicity endpoints are not the result of a broad bacterial sequestration of excess Cu and subsequent reduction in the nematode Cu-body burden.

We also asked whether nematode size could contribute to the observed variation in Cu-body burden. Among Cu-exposed groups, the longer length of *C. elegans* raised on some

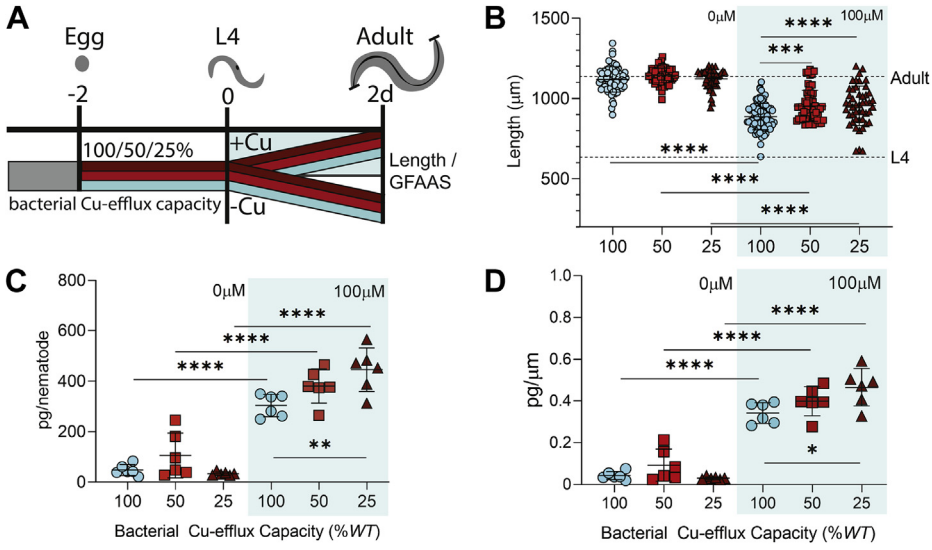

Figure 3. Association between bacterially dependent Cu-sensitivity and *C. elegans* Cu-body burden. *A*, experimental design. All measurements were taken in developmentally synchronous 2d adult populations after 48 h exposure to 0 or 100 μM Cu. *B*, length of developmentally synchronous *N2* nematodes (N = 3–6, n = 7–24). *Dotted lines* represent the average length of nematodes relative to their developmental stage as reported by WormAtlas. *C*, nematode Cu-body burden normalized to pg/nematode (N = 6, n = 20 or 50) (*C*) or (*D*) nematode body burden normalized to average length of nematode population. *Shaded regions* on graphs highlight conditions of excess Cu. Significance was determined by a two-way ANOVA with Tukey's multiple comparisons test. Error bars denote SD and mean. *$p \leq 0.05$. **$p \leq 0.01$. ***$p \leq 0.001$. ****$p < 0.0001$.

bacterial strains could artificially increase the Cu-body burden calculated relative to smaller nematodes when reported as pg/nematode. Nevertheless, using the average length collected at the same timepoint, populations normalized to pg/μm did not fully account for this variation in Cu-body burden (Fig. 3*D*); pg/μm of Cu-body burden increased by nearly 27% (p = 0.0150, two-way ANOVA with Tukey's multiple comparisons), from 0.34 ± 0.05 pg/μm on 100%*WT* to 0.47 ± 0.09 pg/μm when the bacterial lawn retained only 25%*WT* bacterial Cu-efflux capacity. Together, these experiments show that nematode Cu-body burden is not significantly reduced by impairing the bacterial Cu-efflux capacity despite the marked improvement in other toxicity measures in *C. elegans*.

Spatial activation of numr-1 *is dependent on bacterial Cu-efflux capacity*

Since the nematode Cu-body burden did not explain the bacterially dependent Cu resistance in *C. elegans*, we sought to test whether the quality of a nematode metal stress response could account for the variation. To this end, we monitored the expression of a protective metal stress response gene, *numr-1*, which has been associated with improved survival during metal stress as well as reduced MH risk related to neuromuscular function in the vulva (42, 43). We focused on pharyngeal activation of a transgene reporter for *numr-1*, *mtEx60 [numr-1p::GFP + rol-6(su1006)]* (JF85) within a 48 h exposure window (Fig. 4*A*) since activation of this transgene in the pharynx is unique to Cu and not responsive to other environmental challenges such as pathogenic infection, endoplasmic reticulum stress, starvation, or oxidative stress responses (47). Furthermore, pharyngeal filter feeding is responsible for concentrating and breaking down bacteria in *C. elegans*; after expelling extra fluid from the anterior pharynx, the nematode pushes a concentrated bacterial pellet *via* neuromuscular contractions back to the posterior pharynx where pharyngeal grinding disrupts most of the bacteria before passage into the intestine (Fig. 4*B*) (48). Therefore, the intensity and location of *numr-1p::GFP* activation within the nematode pharynx were used to characterize the impact of bacterial Cu-handling dynamics on this metal stress marker.

Under control conditions (0 μM Cu), negligible corrected mean intensities of *numr-1p::GFP* expression were reported in all regions (Fig. S4) and minimal constitutive expression was

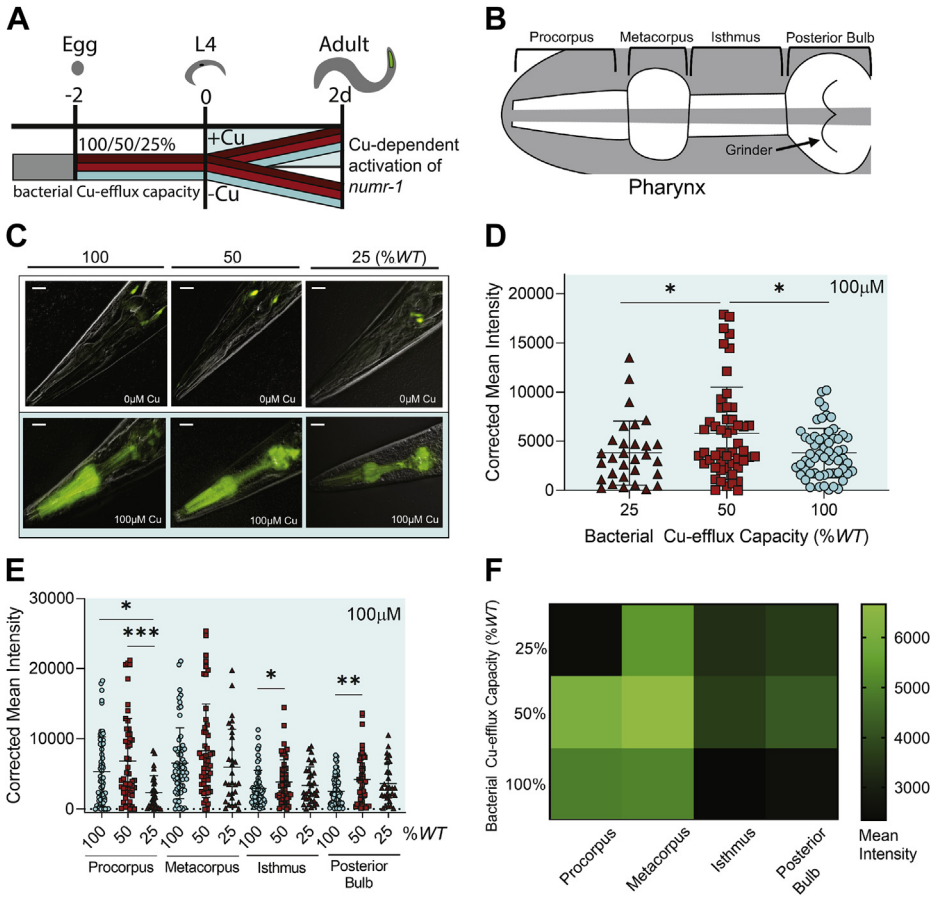

Figure 4. Bacterial Cu-efflux capacity affects Cu-dependent pharyngeal *numr-1* activation. *A*, exposure design prior to GFP transgene imaging. *B*, diagram of nematode pharynx divided into four anatomical regions encompassing the anterior (procorpus and metacorpus) and posterior (isthmus and posterior bulb) pharynx. *C*, representative fluorescence microscopy images of *numr-1p::GFP* responding to 0 μM or 100 μM Cu. Scale bar in *upper right corners* is 20 μm long. *D*, quantification of corrected mean intensity of GFP signal present in the pharynx or (*E*) the separate anatomical regions (N = 4–6, n = 5–12). *Shaded regions* on graphs highlight conditions of 100 μM Cu. A one-way ANOVA with Tukey's multiple comparison analysis was used to determine significance while error bars denote mean and SD. *$p \le 0.05$. ** $p \le 0.01$. ***$p \le 0.001$. *F*, summary heat map of regional mean intensity of GFP signal present in the pharynx when exposed to 100 μM Cu.

noted in the head neurons surrounding the pharynx for all bacterial conditions (Fig. 4*C*). As anticipated, following 100 μM Cu exposure over a 48 h window starting at the L4 stage (Fig. 4*A*), a strong activation of the *numr-1p::GFP* transgene is observed when nematodes are raised in 100%*WT* bacteria (Fig. 4*C*). However, while under Cu stress, transgene activation in the pharynx was variably impacted by reducing the bacterial Cu-efflux capacity; 50%*WT* bacteria resulted in a higher corrected mean intensity than the 100%*WT* control bacteria (p = 0.0127, one-way ANOVA with Tukey's multiple comparisons) while 25%*WT* bacteria had a comparable mean intensity to the 100%*WT* control (p = 0.0455, one-way ANOVA with Tukey's multiple comparisons) (Fig. 4*D*).

The difference in cumulative mean intensity between bacterial conditions also coincided with highly variable transgene activation within the four regions of the pharynx in response to Cu (Fig. 4*C*), suggesting that pharyngeal *numr-1* may be spatially influenced by the bacterial Cu-efflux capacity. Thus, we further analyzed and quantified the spatial regulation of *numr-1p::GFP* expression in the pharynx. Within the anterior pharynx, where diluted bacteria and media are collected from the environment prior to filtration, the nematodes on 25%*WT* bacteria exhibited a significant reduction in the most anterior procorpus compared with either 50 or 100%*WT* bacterial Cu-efflux groups (p = 0.0006 and 0.0256 respectively, one-way ANOVA with Tukey's multiple comparisons). All other corrected mean intensities reported in the regions of the anterior pharynx were unaffected by bacterial Cu-efflux. In contrast, both regions of the posterior pharynx, encompassing the isthmus and posterior bulb, which respectively concentrate and grind the bacterial pellet, exhibited significant increases in the corrected mean intensity for 50%*WT* bacteria compared with 100%*WT* control (isthmus p = 0.0120, posterior bulb p = 0.0067, one-way ANOVA with Tukey's multiple comparisons). Similarly, the levels of posterior transgene activation observed in nematodes on 25%*WT* bacteria compensated for their depressed activation in the procorpus enough to retain similar cumulative mean intensity to 100%*WT* controls (Fig. 4*E*). Visualized in a heat map of the average reported intensities (Fig. 4*F*), these observations show how reduced Cu-efflux capacity shifts the *numr-1* metal stress response posteriorly. In particular, these results suggest that *numr-1* activation in the anterior pharynx is dependent on the environmental concentration of Cu in the media while *numr-1* activation in the posterior pharynx is dependent on the release of bacterially accumulated Cu, which is present at higher levels in bacteria with reduced Cu-efflux capacity.

numr-1 *mediates toxicity responses to bacterially accumulated Cu*

Since spatial activation of *numr-1p::GFP* positively correlated with reduced toxicity, we tested whether the *numr-1* mediated metal stress response is required for bacterially dependent Cu resistance (Fig. 5*A*). To this end, we chose to specifically monitor MH risk since this endpoint shows the most sensitive (*i.e.*, magnitude difference) response between different bacterial Cu-efflux capacities (Fig. 2, *C* and *D*) and because endogenous expression of *numr-1* is also observed in the vulval muscles where maintained function is necessary for egg laying (47). Without Cu, we did not observe a difference in MH risk between WT and *numr-1* loss-of-function mutants (*numr-1(ok2239)*) (Fig. 5, *B* and *D*) despite previous reports of metal-independent increases in MH risk in *numr-1* loss of function mutants (47). However, when Cu was added to the media, a different pattern of MH risk emerged between the *N2* control populations and mutants. While *N2* nematodes raised on bacterial lawns with reduced Cu-efflux capacity still exhibited a significantly reduced MH risk relative to those raised on bacteria with 100%*WT* Cu-efflux capacity during Cu stress (Fig. 5*C*, p = 0.0283, two-way ANOVA with Tukey's multiple comparisons), *numr-1* mutants did not exhibit the same reduction in MH risk in the presence of reduced bacterial Cu-efflux capacity (Fig. 5*C*, p = 0.9839, two-way ANOVA with Tukey's multiple comparisons). Though there is slightly higher Cu-independent MH observed across all bacterial and nematode strain combinations in these matched experimental replicates when compared with earlier experiments, the loss of bacterially dependent protection against MH at later timepoints in *numr-1* (Fig. 5*E*) is consistent with our imaging results and suggests that *numr-1* plays a role in Cu-dependent MH risk associated with bacterial Cu handling. Taken together, these results indicate that the expression of *numr-1* in *C. elegans* plays a role in the decreased Cu-toxicity response observed when the bacterial Cu-efflux capacity is reduced.

Discussion

Cu excess is a condition that organisms have evolved to counteract for millions of years. Without the prospect of degradation, homeostatic responses and methods of detoxification through chelation are deeply conserved across phyla. Though it is understood that single-celled and multicellular organisms respond to environmental challenges such as Cu excess (13, 49, 50), the coordination between organisms exposed to the same environmental challenge has not been thoroughly explored. In this work, we used a simplified host–microbe system to isolate the contribution of a ubiquitous bacterial response to Cu stress (Fig. 1). We found that increasing bacterial Cu-efflux capacity drives increased sensitivity to Cu stress in the host nematode (Fig. 2). Without the addition of 100 μM Cu in the media, the contribution of bacterial Cu-efflux capacity is negligible to nematode life span (Fig. 2*B*), MH risk (Fig. 2*C*), length (Fig. 3*B*) and Cu-body burden (Fig. 3, *C* and *D*). However, when 100 μM Cu is present in the media, the contribution of bacterial Cu-efflux becomes a major determinant of life span (Fig. 2*B*) and MH risk (Fig. 2*D*) over time. Rather than an increase in Cu-body burden (Fig. 3, *C* and *D*) driving sensitization in the nematode, worsened outcomes during Cu stress coincide with reduced activation of a protective metal-responsive gene in the posterior pharynx (Fig. 4*E*). Reduced activation of this gene localized to the procorpus and increased activation localized to the isthmus and posterior bulb (Fig. 4*F*) of the pharynx identify

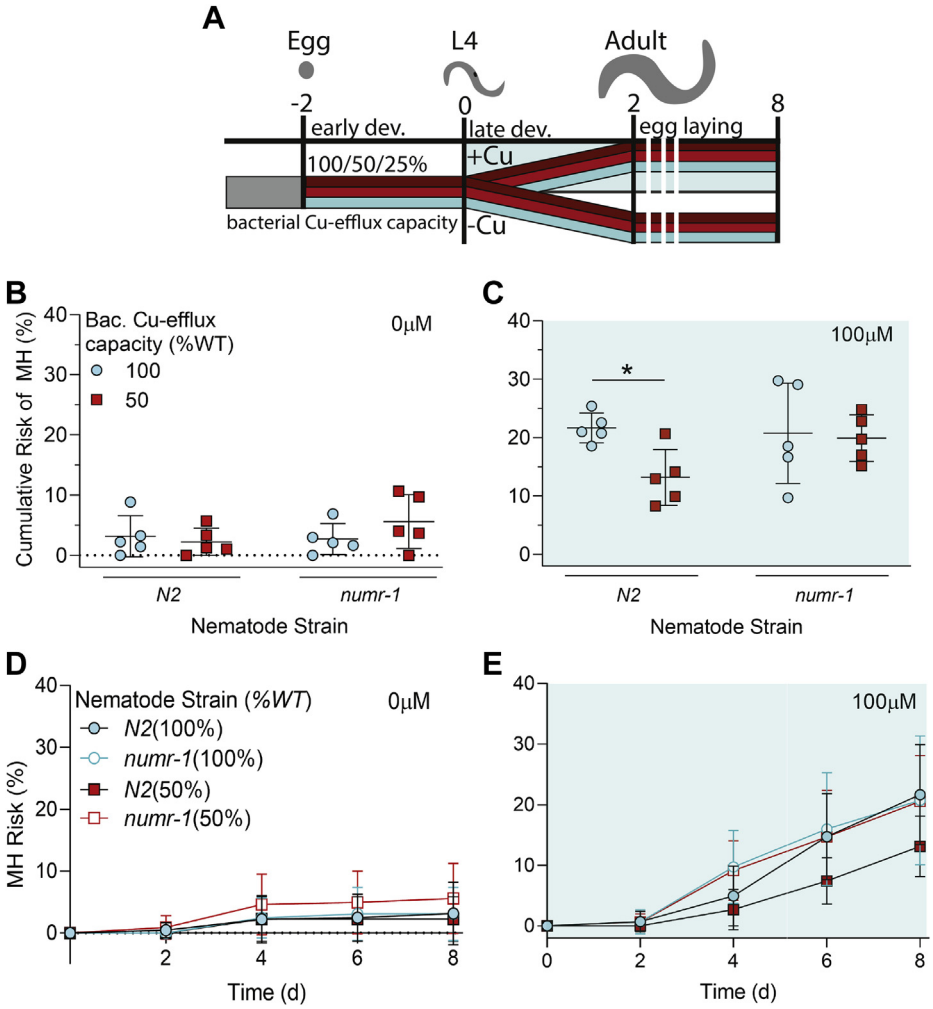

Figure 5. *numr-1* involvement in bacterially dependent Cu resistance. *A*, experimental design. Cumulative MH risk of experimentally matched *N2* nematodes and *numr-1* nematodes with an impaired *numr-1* response in (*B*) 0 μM or (*C*) 100 μM Cu (N = 5, n = 62–134). *Shaded regions* on graphs highlight conditions of 100 μM Cu. A two-way ANOVA with Tukey's multiple comparison analysis was used to determine significance while error bars denote mean and SD and $*p \leq 0.05$.

bacterial Cu-efflux capacity as a spatial determinant of the host nematode's early metal stress response system. Without this effective early metal stress response system, bacterially dependent Cu resistance observed in MH risk was no longer present during 100 μM Cu exposures (Fig. 5). These results support a model whereby an environment's bacterial Cu-efflux capacity determines the activation of the host nematode *numr-1*-mediated metal stress response and the development of subsequent Cu-toxicity endpoints (Fig. 6).

Disconnecting dose-dependent toxicity in the host

We assessed the impact of bacterial Cu resistance on the Cu-homeostatic system in *C. elegans*. The removal or silencing of Cu-homeostatic elements reduces Cu-body burden in nematodes while increasing the severity of Cu-toxicity endpoints at higher concentration of environmental Cu (31, 32). Without genetic silencing of Cu homeostatic elements in nematodes, the free waterborne fraction of Cu in the environment was shown to be the most significant contributor to the Cu-body burden and subsequent toxicity in conditions of Cu excess (33, 40). While the potential role for bacterially associated Cu is recognized, the impact was considered minimally additive to the body-burden and toxicity of free waterborne exposures (35, 38). Our work assesses the significance of bacterially accumulated Cu in a host–microbe system. The protective quality of a reduced bacterial Cu-efflux capacity in the *C. elegans*/*E. coli* system challenges the previous assumption that bacterially accumulated and waterborne Cu have similar additive effects on nematode toxicity. We determined whether altered Cu bioavailability or the nematode's homeostatic response contributed to the variable toxicity observed between bacterial strains during Cu stress; rather than bacterially accumulated Cu being less bioavailable, reducing the Cu-body burden concurrently with Cu toxicity *in vivo*, the observed dissociation of Cu-body burden from other Cu-toxicity endpoints suggests that the nematode's own homeostatic response to Cu is responsive to bacterial Cu-handling.

However, excess Cu elicits a range of transcriptomic and behavioral responses that may contribute to organismal Cu

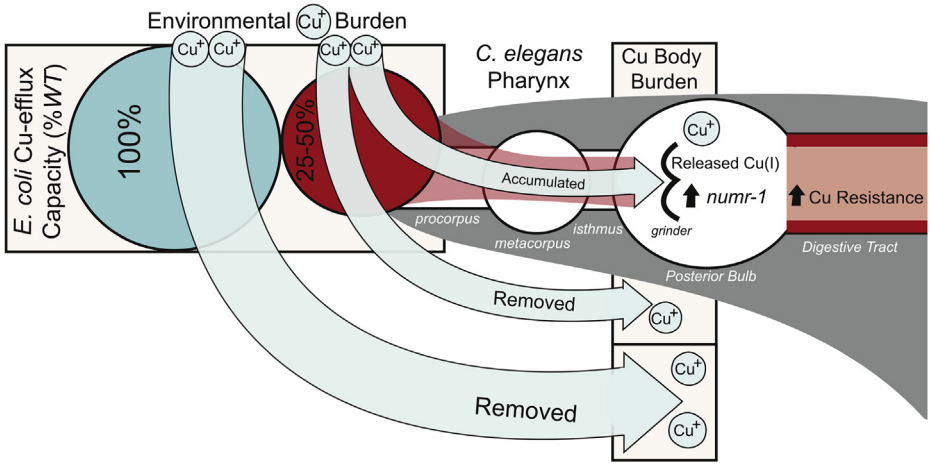

Figure 6. Bacterial Cu-efflux capacity acts spatially on host response to environmental metal stress. The efficiency of bacterial Cu efflux, during conditions of metal excess, alters the spatial distribution of metal stress in host organisms. Specifically, increasing bacterial Cu-efflux capacity reduces the protective upregulation of the host's metal-responsive *numr-1* by reducing the fraction of bacterially-accumulated Cu in the posterior bulb. When bacterial Cu-efflux capacity is reduced, subsequently increased activation of metal-responsive *numr-1* contributes to improved Cu-toxicity endpoints in the host without reducing the host's overall Cu-body burden.

toxicity related to longevity, MH risk, and development. For instance, the late MH risk associated with Cu toxicity (Fig. 2*D*) can also be seen after periods of starvation beginning at L4 (48). *C. elegans* MH has been proposed as a model for myometrial degeneration (51), a disorder that manifests in conditions of Cu excess and misregulation, as reported here, and associates with spontaneous miscarriage for women afflicted with Wilson's disease, a disorder of impaired Cu homeostasis that results in widespread Cu toxicity (52). Other factors that can cause an increased MH risk include high salt, pathogen infection, and developmental defects (48). However, these factors typically associate with earlier MH than what is reported here (Fig. 2*D*). Therefore, future work with altered bacterial Cu-efflux capacities will serve to 1) identify the variety of transcriptomic responses in the nematode impacted before and after Cu stress and 2) determine the extent to which the bacterial Cu-efflux capacity alters perceived food quality, which may contribute to the development of starvation. For example, reductions in pharyngeal pumping in response to increasing Cu concentrations in the media or changes to food quality and quantity could contribute to starvation-associated MH (35, 38, 47). Similarly, behavioral aversion to media Cu concentrations does not appear significant in the literature until around 200 μM, which suggests that altered bioavailability of the metal due to differing bacterial Cu-efflux rates would not greatly increase the nematodes aversion response to feeding in our model (31). Perceived and functional food deprivation studies through these means can determine whether starvation or aversion responses contribute to the Cu-toxicity endpoints that are modified by the bacterial Cu-efflux capacity.

Pharyngeal signal for protective Cu-stress response

Researchers previously identified the intestinal tract as the major contributor to Cu homeostasis in *C. elegans*, in line with what is known of other organisms such as mice and humans (20, 32). This conclusion was supported by the ability of intestine-specific expression of an ATP7A/B homolog to rescue mutant nematodes during Cu deficiency. However, expression of the same homolog within the pharyngeal region implied that this organ may play a role in Cu homeostasis (32). The Cu-specific pharyngeal activation of *numr-1p::GFP*, dependent on the bacterial Cu-efflux capacity, reported here further supports the pharynx as an organ involved in Cu homeostasis. Furthermore, *numr-1* expression was previously reported to be protective against metal-specific toxicity induced by RNA-processing errors (42, 47). Our work also expands upon this research by reporting on the unexpected impact of bacterial Cu-efflux on the spatial distribution of this metal-specific response; bacterially accumulated Cu has a greater impact on *numr-1* posterior pharyngeal expression while the media concentration appears to have a stronger influence on the anterior pharynx (Fig. 4). Our results demonstrate the significance of regional variation in microbial composition and function in the digestive tract of higher organisms (20). Despite the ubiquitous expression of microbial Cu-resistance genes across the digestive tract (23), the developmental timing and early localization of this activity may serve to inform the subsequent host responses to excess metal.

Implications of bacterial Cu resistance

Bacterial Cu-resistance has evolved in response to increasing widespread anthropogenic release of Cu into the environment (22). Gene clusters conferring this resistance often persist and undergo horizontal gene transfer among Enterobacteriaceae that require stronger resistance to survive changing environments (21). However, the consequences of this shift in a host–microbe system have not been documented. Using a simplified host–microbe system, we found that increasing one aspect of bacterial Cu resistance, conferred by the Cus system, sensitized the host to Cu toxicity independent of an increased Cu-body burden (Figs. 2 and 3) and

disrupts the efficacy of a host metal-specific stress response *in vivo* (Figs. 4 and 5). Nevertheless, while the Cus system is particularly important for conferring Cu resistance in anaerobic environments through Cu removal, it does not act in isolation. For instance, the plasmid-borne Cu-resistance system (*pco*), homologous to the Cu-resistance operon (*cop*) in *Pseudomonas*, serves to detoxify intracellular Cu rather than remove it from the cell (21, 53). Earlier experiments in host–microbe interactions using *C. elegans* found that bacterial mutations that induce free radical detoxification in bacteria activated mitochondrial stress responses nematodes (28). Our own experiments suggest that variations in baseline and early MH, independent of Cu stress, may result from the unique disruption of the H_2O_2 response pathway in *E. coli* (Fig. 2*D*). Together, these experiments highlight the unexpected consequences of increasingly Cu-resistant microbial populations in the environment and describe how one aspect of bacterial Cu resistance, Cu-efflux capacity, spatially modulates host metal stress responses.

Experimental procedures

C. elegans *genetics and strains*

All *C. elegans* strains were obtained from the *Caenorhabditis* Genetic Center (CGC). Only nonstarved cultures maintained on *OP50* at 20 °C on nematode growth media (NGM: 3 g NaCl, 17 g agar, 2.5 g peptone, 1 ml 1 M $CaCl_2$, 1 ml 5 mg/ml cholesterol in ethanol, 1 ml 1 M $MgSO_4$, 25 ml 1 M KPO_4 per liter) were used for all downstream experiments. The *C. elegans* strains used were:

- *N2*: wild-type for all general toxicity endpoints
- *JF85*: mtEx60 [numr-1p::GFP + rol-6(su1006)] for visualization of a metal stress-specific transgene
- *RB1749*: *numr-1(ok2239)* III for matricidal-hatching experiments.

E. coli *genetics and strains*

E. coli strains were either ordered from the CGC or previously isolated and characterized (1, 2) in which established methods were used to disrupt targeted chromosomal genes. The *E. coli* strains used were:

- *OP50 -E. coli* B uracil auxotroph
- *WT* -BW25113/*ΔcueO*::catR/pET21b(+), control, 100%*WT* bacterial Cu-efflux capacity
- *ΔcusS* -BW25113/*ΔcueOΔcusS*/pET21b(+), 50%*WT* bacterial Cu-efflux capacity
- *ΔcusR* -BW25113/*ΔcueOΔcusR*/pET21b(+) (1), 25%*WT* bacterial Cu-efflux capacity
- *E. coli BL21(DE3)*, pLIC-egfp inducible expression

All *E. coli* strains except *OP50* and *BL21(DE3)* were maintained at 4 °C as single colony plates on Luria broth agar (10 g bacto-tryptone, 10 g NaCl, 5 g yeast extract, 15 g bacto-agar per liter) supplemented with 5 μl 100 ng/ml ampicillin. *OP50* and *BL21(DE3)* were maintained on Luria broth agar without ampicillin.

Bacterial culture conditions

Bacterial lawns were prepared by growing overnight cultures at 37 °C from a single colony then normalizing to 1×10^8 cells/ml before pipetting 200 μl of culture onto the appropriate NGM plates. Seeded plates were incubated at room temperature for 48 h prior to storage at 4 °C.

Bacterial growth rate and plate density

For each bacterial strain, a single colony was grown overnight at 37 °C. From this overnight culture, a 1:100 dilution was made with fresh LB to reach a starting concentration of 0.05 OD_{600}. The OD_{600} was measured every 30 min until 0.1 was reached. The culture was then diluted by 1:20 with LB containing the desired amount of $CuSO_4$. The OD_{600} in this culture was measured every hour through exponential growth until the stationary phase was observed. Plate density was determined following a 48 h incubation after plates were seeded. Two milliliters of media was used to wash plates of bacterial lawn and diluted 1:100 before OD_{600} quantification.

Exposure conditions

Dosage was chosen based on previously described 1) dose-dependent toxicity endpoints and EC50 values in the host nematode 2) concentrations relevant to environmental exposures reported globally and 3) dosage studies reporting acute digestive distress upon oral administration in humans and 4) at a concentration that would not impact survival or growth of the *E. coli* strains (25, 32, 33, 35, 54–56). All Cu exposures were prepared by adding 0 μM or 100 μM $CuSO_4$ to NGM agar immediately prior to pouring the media plates. Developmentally synchronous populations of *C. elegans* used for toxicity endpoint analysis were obtained from nonstarved *OP50* maintenance plates through the use of hypochlorite bleach egg selection (57). In addition to synchronizing populations, hypochlorite bleaching allowed for direct and sterile transfer of eggs from maintenance plates to those that had been seeded with other *E. coli* strains instead. A second transfer 48 h after bleach synchronization allowed for a population of nematodes to begin exposure to ±$CuSO_4$ at the L4 developmental stage.

Length determination

Nematode length was measured 48 h post L4 transfer to ±Cu plates. For each of the independent experiments, approximately 12 adults from each condition were washed with M9 buffer (3 g KH_2PO_4, 6 g Na_2HPO_4, 5 g NaCl, 1 ml 1 M $MgSO_4$ per liter) (58) and placed on bacteria-free NGM. The nematodes were recorded for 15 s while roaming around the plate. Video analysis using WormLab tracking software was used to quantify average length for each worm from head to tail.

Body-burden measurements

Forty-eight hours after ±Cu exposure starting at L4, 20 to 50 adult nematodes from each plate were collected for

metal-content analysis as previously described (59). Briefly, *C. elegans* were moved to unseeded NGM plate before being transferred to a 1.5 ml microfuge tube containing 200 µl M9 buffer. Microfuge tubes were rotated by inversion continually for at least 30 min to remove excess bacteria. After the first incubation, worms were washed three times with 200 µl M9 buffer and three times with ddH_2O to effectively remove all traces of residual bacteria. The supernatant was removed between each wash under a stereomicroscope to prevent sample loss. Following the last wash, samples were flash frozen in liquid nitrogen and desiccated using an SPD1010 SpeedVac vacuum concentrator. In total, 20 µl of 70% HNO_3 was added to desiccated samples before incubation at room temperature overnight followed by a 1 h incubation at 60 °C the next morning to fully digest the pellet. In total, 380 µl of 1% HNO_3 was added to samples for a final HNO_3 concentration of 4%. Prepared samples were analyzed for Cu content using GFAAS and run in triplicate before the average concentration was determined from an established calibration curve. Body burden is reported as pg/nematode or pg/µm after normalizing for nematode size

Lethality

All lethality experiments were conducted as previously described in *N2 C. elegans* transferred from bleach synchronized populations at L4 to exposure conditions after preconditioning of the bacterial condition following bleach synchronization in early development (60). With the exception of the 36 h timepoint after transfer to the exposure condition, all nematodes were transferred every 48 h to new plates to keep generations distinguishable while the nematode was still egg laying and then to prevent starvation at later stages of the lethality experiments. Lethality was tested at least every 48 h using a worm pick to look for a touch response. If no movement or response is detected, the nematodes were presumed dead and recorded as such. Nematode populations were simultaneously assessed to account for censorship *via* disappearance from the plate, MH, everted vulva, or death resulting from worm pick or transfer. Kaplan–Meier curve analysis was conducted on collected data to determine significant differences between groups.

Cumulative population risk of matricidal hatching

Occurrence of MH in a population was assessed every 48 h for 7 days after L4 transfer to ±Cu plates under a dissecting microscope through the reproductive period of the nematode. Analysis of data used a cumulative incidence model to adjust for a smaller population over time caused by death or censored *C. elegans* not attributable to a bagging phenotype. For every 48 h period, the cumulative incidence was divided by the number of subjects at risk in the population at the beginning of the period. Multiplying for the duration of each population's active reproductive period where the majority of bagging occurs (about 7.5 days) gives total cumulative risk among replicate populations. Five to eight independent experiments of 25 to 30 nematodes were conducted for each conditional exposure. A modified Kaplan–Meier risk assessment was used to measure this parameter to minimize the effect of variable survival in the populations (60); for instance, a smaller population as a result of increased death in one condition could artificially reduce incidence of MH observed if the actual population at risk is not accounted for at each timepoint.

Brood-size measurement

Viable brood size was assessed on an individual basis: one nematode was placed in ±Cu plates with the preconditioned bacteria at the L4 stage. Thirty-six hours after initial transfer each nematode was transferred to a new plate. Transfers to new plates were performed every 24 h after the initial 36 h transfer. After 30 min at 4 °C to slow movement, each progeny plate was counted 2 days after the initial egg lay before the F1 began to produce progeny. Each bacterial/Cu condition was tested with three independent replicates composed of five individual nematode replicates.

Imaging

Before imaging, *C. elegans* exposure and control groups were derived from the same bleach-synchronized population for each bacterial condition and exposed in late development for 48 h from L4 to early adulthood. Nematodes were then incubated in 100 µM levamisole to inhibit movement while pharyngeal images were taken at 40x using a Nikon H600L fluorescence microscope with uniform exposure times and Z-stack width and processing. The GFP induction was quantified using ImageJ 1.52p for each pharyngeal region. Images taken with a different camera were normalized using the signal to background ratio calculated with an identical sample imaged on both camera set ups. Corrected mean intensity was calculated by subtracting normalized background signals from all samples before subtracting the corrected mean intensity of 0 µM Cu controls from the matched 100 µM mean intensity for each experimental replicate.

Statistical analysis

Experimental designs are reported in figure legends such that N=independent experimental replicates and n=biological replicates in each experimental replicate. All statistical analysis was performed in GraphPad Prism (v8.2.0). For life span analyses, a log-rank Mantel–Cox test was used to calculate significance. Significant interactions were analyzed for cumulative MH risk, Cu-body burden, brood size, and length. An ordinary one-way ANOVA with Tukey's multiple comparison test was used to analyze interactions between *numr-1p::GFP* transgene activation and bacterial Cu-efflux capacity. A two-way ANOVA with Tukey's multiple comparison's test was also used to confirm that sample size did not account for variation in Cu-body burden determination.

Data availability

All data are available within the article and supporting information.

Supporting information—This article contains supporting information.

Author contributions—C. M. S. and M. M. M. conceptualization; C. M. S. and A. T. data curation; C. M. S. formal analysis; C. M. S. and M. M. M. funding acquisition; C. M. S. and A. T. investigation; C. M. S., A. T., P. A., and M. M. M. methodology; C. M. S., P. A., and M. M. M. project administration; P. A. and M. M. M. resources; P. A. and M. M. M. software; P. A. and M. M. M. supervision; C. M. S. and A. T. validation; C. M. S. visualization; C. M. S. writing-original draft; C. M. S., P. A., and M. M. M. writing-review and editing.

Funding and additional information—P.A. is supported by NIEHS R01 ES027487. C.M.S. was supported by the NIEHS T32 training grant "Training in Molecular Toxicology" T32ES015457. The content is solely the responsibility of the authors and does not necessarily represent the official views of the National Institutes of Environmental Health Sciences.

Conflict of interest—The authors declare that they have no conflicts of interest with the contents of this article.

Abbreviations—The abbreviations used are: Cu, copper; GFAAS, graphite furnace atomic absorption spectroscopy; MH, matricidal hatching; NGM, nematode growth media; TCS, two-component system.

References

1. Pryor, R., Norvaisas, P., Marinos, G., Best, L., Thingholm, L. B., Quintaneiro, L. M., De Haes, W., Esser, D., Waschina, S., Lujan, C., Smith, R. L., Scott, T. A., Martinez-Martinez, D., Woodward, O., Bryson, K., *et al.* (2019) Host-microbe-drug-nutrient screen identifies bacterial effectors of metformin therapy. *Cell* **178**, 1299–1312.e1229
2. Scott, T. A., Quintaneiro, L. M., Norvaisas, P., Lui, P. P., Wilson, M. P., Leung, K. Y., Herrera-Dominguez, L., Sudiwala, S., Pessia, A., Clayton, P. T., Bryson, K., Velagapudi, V., Mills, P. B., Typas, A., Greene, N. D. E., *et al.* (2017) Host-microbe co-metabolism dictates cancer drug efficacy in C. elegans. *Cell* **169**, 442–456.e418
3. Javdan, B., Lopez, J. G., Chankhamjon, P., Lee, Y. J., Hull, R., Wu, Q., Wang, X., Chatterjee, S., and Donia, M. S. (2020) Personalized mapping of drug metabolism by the human gut microbiome. *Cell* **181**, 1661–1679.e1622
4. Tan, M. W., and Shapira, M. (2011) Genetic and molecular analysis of nematode-microbe interactions. *Cell. Microbiol.* **13**, 497–507
5. Watson, E., MacNeil, L. T., Ritter, A. D., Yilmaz, L. S., Rosebrock, A. P., Caudy, A. A., and Walhout, A. J. (2014) Interspecies systems biology uncovers metabolites affecting C. elegans gene expression and life history traits. *Cell* **156**, 759–770
6. Dutta, S. K., Verma, S., Jain, V., Surapaneni, B. K., Vinayek, R., Phillips, L., and Nair, P. P. (2019) Parkinson's disease: The emerging role of gut dysbiosis, antibiotics, probiotics, and fecal microbiota transplantation. *J. Neurogastroenterol. Motil.* **25**, 363–376
7. Hill-Burns, E. M., Debelius, J. W., Morton, J. T., Wissemann, W. T., Lewis, M. R., Wallen, Z. D., Peddada, S. D., Factor, S. A., Molho, E., Zabetian, C. P., Knight, R., and Payami, H. (2017) Parkinson's disease and Parkinson's disease medications have distinct signatures of the gut microbiome. *Mov. Disord.* **32**, 739–749
8. Brown, E., Tanner, C., and Goldman, S. (2018) The microbiome in neurodegenerative disease. *Curr. Geriatr. Rep.* **7**, 81–91
9. Geng, H., Shu, S., Dong, J., Li, H., Xu, C., Han, Y., Hu, J., Han, Y., Yang, R., and Cheng, N. (2018) Association study of gut flora in Wilson's disease through high-throughput sequencing. *Medicine (Baltimore)* **97**, e11743
10. Le Pennec, G., and Ar Gall, E. (2019) The microbiome of Codium tomentosum: Original state and in the presence of copper. *World J. Microbiol. Biotechnol.* **35**, 167
11. Bondarczuk, K., and Piotrowska-Seget, Z. (2013) Molecular basis of active copper resistance mechanisms in Gram-negative bacteria. *Cell Biol. Toxicol.* **29**, 397–405
12. Yamamoto, K., and Ishihama, A. (2005) Transcriptional response of Escherichia coli to external copper. *Mol. Microbiol.* **56**, 215–227
13. Boal, A. K., and Rosenzweig, A. C. (2009) Structural biology of copper trafficking. *Chem. Rev.* **109**, 4760–4779
14. Petris, M. J., Smith, K., Lee, J., and Thiele, D. J. (2003) Copper-stimulated endocytosis and degradation of the human copper transporter, hCtr1. *J. Biol. Chem.* **278**, 9639–9646
15. Dupont, C. L., Grass, G., and Rensing, C. (2011) Copper toxicity and the origin of bacterial resistance–new insights and applications. *Metallomics* **3**, 1109–1118
16. Ala, A., Walker, A. P., Ashkan, K., Dooley, J. S., and Schilsky, M. L. (2007) Wilson's disease. *Lancet* **369**, 397–408
17. Vallières, C., Holland, S. L., and Avery, S. V. (2017) Mitochondrial ferredoxin determines vulnerability of cells to copper excess. *Cell Chem. Biol.* **24**, 1228–1237.e1223
18. Gupte, A., and Mumper, R. J. (2009) Elevated copper and oxidative stress in cancer cells as a target for cancer treatment. *Cancer Treat. Rev.* **35**, 32–46
19. Bourassa, M. W., Leskovjan, A. C., Tappero, R. V., Farquhar, E. R., Colton, C. A., Van Nostrand, W. E., and Miller, L. M. (2013) Elevated copper in the amyloid plaques and iron in the cortex are observed in mouse models of Alzheimer's disease that exhibit neurodegeneration. *Biomed. Spectrosc. Imaging* **2**, 129–139
20. Miller, K. A., Vicentini, F. A., Hirota, S. A., Sharkey, K. A., and Wieser, M. E. (2019) Antibiotic treatment affects the expression levels of copper transporters and the isotopic composition of copper in the colon of mice. *Proc. Natl. Acad. Sci. U. S. A.* **116**, 5955–5960
21. Staehlin, B. M., Gibbons, J. G., Rokas, A., O'Halloran, T. V., and Slot, J. C. (2016) Evolution of a heavy metal homeostasis/resistance island reflects increasing copper stress in enterobacteria. *Genome Biol. Evol.* **8**, 811–826
22. Xing, C., Chen, J., Zheng, X., Chen, L., Chen, M., Wang, L., and Li, X. (2020) Functional metagenomic exploration identifies novel prokaryotic copper resistance genes from the soil microbiome. *Metallomics* **12**, 387–395
23. Segata, N., Haake, S. K., Mannon, P., Lemon, K. P., Waldron, L., Gevers, D., Huttenhower, C., and Izard, J. (2012) Composition of the adult digestive tract bacterial microbiome based on seven mouth surfaces, tonsils, throat and stool samples. *Genome Biol.* **13**, R42
24. Gudipaty, S. A., Larsen, A. S., Rensing, C., and McEvoy, M. M. (2012) Regulation of Cu(I)/Ag(I) efflux genes in Escherichia coli by the sensor kinase CusS. *FEMS Microbiol. Lett.* **330**, 30–37
25. Affandi, T., Issaian, A. V., and McEvoy, M. M. (2016) The structure of the periplasmic sensor domain of the histidine kinase CusS shows unusual metal ion coordination at the dimeric interface. *Biochemistry* **55**, 5296–5306
26. Affandi, T., and McEvoy, M. M. (2019) Mechanism of metal ion-induced activation of a two-component sensor kinase. *Biochem. J.* **476**, 115–135
27. Conroy, O., Kim, E.-H., McEvoy, M. M., and Rensing, C. (2010) Differing ability to transport nonmetal substrates by two RND-type metal exporters. *FEMS Microbiol. Lett.* **308**, 115–122
28. Govindan, J. A., Jayamani, E., Zhang, X., Mylonakis, E., and Ruvkun, G. (2015) Dialogue between E. coli free radical pathways and the mitochondria of C. elegans. *Proc. Natl. Acad. Sci. U. S. A.* **112**, 12456–12461
29. Kishimoto, S., Uno, M., Okabe, E., Nono, M., and Nishida, E. (2017) Environmental stresses induce transgenerationally inheritable survival advantages via germline-to-soma communication in Caenorhabditis elegans. *Nat. Commun.* **8**, 14031

30. Martinez-Finley, E. J., and Aschner, M. (2011) Revelations from the nematode Caenorhabditis elegans on the complex interplay of metal toxicological mechanisms. *J. Toxicol.* **2011**, 895236
31. Yuan, S., Sharma, A. K., Richart, A., Lee, J., and Kim, B. E. (2018) CHCA-1 is a copper-regulated CTR1 homolog required for normal development, copper accumulation, and copper-sensing behavior in Caenorhabditis elegans. *J. Biol. Chem.* **293**, 10911–10925
32. Chun, H., Sharma, A. K., Lee, J., Chan, J., Jia, S., and Kim, B. E. (2017) The intestinal copper exporter CUA-1 is required for systemic copper homeostasis in Caenorhabditis elegans. *J. Biol. Chem.* **292**, 1–14
33. Calafato, S., Swain, S., Hughes, S., Kille, P., and Stürzenbaum, S. R. (2008) Knock down of Caenorhabditis elegans cutc-1 exacerbates the sensitivity toward high levels of copper. *Toxicol. Sci.* **106**, 384–391
34. Anderson, G. L., Boyd, W. A., and Williams, P. L. (2001) Assessment of sublethal endpoints for toxicity testing with the nematode Caenorhabditis elegans. *Environ. Toxicol. Chem.* **20**, 833–838
35. Boyd, W. A., Cole, R. D., Anderson, G. L., and Williams, P. L. (2003) The effects of metals and food availability on the behavior of Caenorhabditis elegans. *Environ. Toxicol. Chem.* **22**, 3049–3055
36. Boyd, W. A., and Williams, P. L. (2003) Comparison of the sensitivity of three nematode species to copper and their utility in aquatic and soil toxicity tests. *Environ. Toxicol. Chem.* **22**, 2768–2774
37. Harrington, J. M., Boyd, W. A., Smith, M. V., Rice, J. R., Freedman, J. H., and Crumbliss, A. L. (2012) Amelioration of metal-induced toxicity in Caenorhabditis elegans: Utility of chelating agents in the bioremediation of metals. *Toxicol. Sci.* **129**, 49–56
38. Mashock, M. J., Zanon, T., Kappell, A. D., Petrella, L. N., Andersen, E. C., and Hristova, K. R. (2016) Copper oxide nanoparticles impact several toxicological endpoints and cause neurodegeneration in Caenorhabditis elegans. *PLoS One* **11**, e0167613
39. Twumasi-Boateng, K., Wang, T. W., Tsai, L., Lee, K. H., Salehpour, A., Bhat, S., Tan, M. W., and Shapira, M. (2012) An age-dependent reversal in the protective capacities of JNK signaling shortens Caenorhabditis elegans lifespan. *Aging Cell* **11**, 659–667
40. Moyson, S., Town, R. M., Joosen, S., Husson, S. J., and Blust, R. (2019) The interplay between chemical speciation and physiology determines the bioaccumulation and toxicity of Cu(II) and Cd(II) to Caenorhabditis elegans. *J. Appl. Toxicol.* **39**, 282–293
41. Richards, A. L., Watza, D., Findley, A., Alazizi, A., Wen, X., Pai, A. A., Pique-Regi, R., and Luca, F. (2017) Environmental perturbations lead to extensive directional shifts in RNA processing. *PLoS Genet.* **13**, e1006995
42. Wu, C. W., Wimberly, K., Pietras, A., Dodd, W., Atlas, M. B., and Choe, K. P. (2019) RNA processing errors triggered by cadmium and integrator complex disruption are signals for environmental stress. *BMC Biol.* **17**, 56
43. Kimble, J. E., and White, J. G. (1981) On the control of germ cell development in Caenorhabditis elegans. *Dev. Biol.* **81**, 208–219
44. Shin, N., Cuenca, L., Karthikraj, R., Kannan, K., and Colaiácovo, M. P. (2019) Assessing effects of germline exposure to environmental toxicants by high-throughput screening in C. elegans. *PLoS Genet.* **15**, e1007975
45. Urano, H., Umezawa, Y., Yamamoto, K., Ishihama, A., and Ogasawara, H. (2015) Cooperative regulation of the common target genes between H(2)O(2)-sensing YedVW and Cu(2)(+)-sensing CusSR in Escherichia coli. *Microbiology (Reading)* **161**, 729–738
46. Angelo, G., and Van Gilst, M. R. (2009) Starvation protects germline stem cells and extends reproductive longevity in C. elegans. *Science* **326**, 954
47. Tvermoes, B. E., Boyd, W. A., and Freedman, J. H. (2010) Molecular characterization of numr-1 and numr-2: Genes that increase both resistance to metal-induced stress and lifespan in Caenorhabditis elegans. *J. Cell Sci.* **123**, 2124–2134
48. Chen, J., and Caswell-Chen, E. P. (2004) Facultative vivipary is a life-history trait in Caenorhabditis elegans. *J. Nematol.* **36**, 107–113
49. Djaman, O., Outten, F. W., and Imlay, J. A. (2004) Repair of oxidized iron-sulfur clusters in Escherichia coli. *J. Biol. Chem.* **279**, 44590–44599
50. Milne, L., Nicotera, P., Orrenius, S., and Burkitt, M. J. (1993) Effects of glutathione and chelating agents on copper-mediated DNA oxidation: Pro-oxidant and antioxidant properties of glutathione. *Arch. Biochem. Biophys.* **304**, 102–109
51. Pickett, C. L., and Kornfeld, K. (2013) Age-related degeneration of the egg-laying system promotes matricidal hatching in Caenorhabditis elegans. *Aging Cell* **12**, 544–553
52. Malik, A., Khawaja, A., and Sheikh, L. (2013) Wilson's disease in pregnancy: Case series and review of literature. *BMC Res. Notes* **6**, 421
53. Brown, N. L., Barrett, S. R., Camakaris, J., Lee, B. T., and Rouch, D. A. (1995) Molecular genetics and transport analysis of the copper-resistance determinant (pco) from Escherichia coli plasmid pRJ1004. *Mol. Microbiol.* **17**, 1153–1166
54. Ahmad, J. U., and Goni, M. A. (2010) Heavy metal contamination in water, soil, and vegetables of the industrial areas in Dhaka, Bangladesh. *Environ. Monit. Assess.* **166**, 347–357
55. Knobeloch, L., Ziarnik, M., Howard, J., Theis, B., Farmer, D., Anderson, H., and Proctor, M. (1994) Gastrointestinal upsets associated with ingestion of copper-contaminated water. *Environ. Health Perspect.* **102**, 958–961
56. Stenhammar, L. (1999) Diarrhoea following contamination of drinking water with copper. *Eur. J. Med. Res.* **4**, 217–218
57. Rehman Khan, F., and McFadden, B. A. (1980) A rapid method of synchronizing developmental stages of Caenorhabditis elegans. *Nematologica* **26**, 280–282
58. Brenner, S. (1974) The genetics of Caenorhabditis elegans. *Genetics* **77**, 71–94
59. Ganio, K., James, S. A., Hare, D. J., Roberts, B. R., and McColl, G. (2016) Accurate biometal quantification per individual Caenorhabditis elegans. *Analyst* **141**, 1434–1439
60. Amrit, F. R., Ratnappan, R., Keith, S. A., and Ghazi, A. (2014) The C. elegans lifespan assay toolkit. *Methods* **68**, 465–475